sustainability

MDPI

Article

Catalytic Effects of Potassium Concentration on Steam Gasification of Biofuels Blended from Olive Mill Solid Wastes and Pine Sawdust for a Sustainable Energy of Syngas

Chafaa Nsibi [1], Victor Pozzobon [2,*], Javier Escudero-Sanz [3] and Marzouk Lajili [1]

[1] EMIR (Etude des Milieux Ionisés et Réactifs) Laboratory, Monastir University, 15 Avenue Ibn Eljazzar IPEIM, Monastir 5019, Tunisia; chafaa23@hotmail.com (C.N.); marzouk.lajili@ipeim.rnu.tn (M.L.)
[2] Centre Européen de Biotechnologie et de Bioéconomie (CEBB), Laboratoire de Génie des Procédés et Matériaux, Centrale Supélec, Université Paris-Saclay, 3 rue des Rouges Terres, 51110 Pomacle, France
[3] Ecole des Mines Albi-Carmaux, RAPSODEE Laboratory, Campus Jarlard, CEDEX 09, 81013 Albi, France; javier.escuderosanz@mines-albi.fr
* Correspondence: victor.pozzobon@centralesupelec.fr

Abstract: The effect of potassium impregnation at different concentrations during gasification, under nitrogen/water steam atmosphere, of char produced via pyrolysis of olive mill residues blended or not with pine sawdust was investigated. Three concentrations (0.1 M, 0.5 M, and 1.5 M) of potassium carbonate solution (K_2CO_3) were selected to impregnate samples. First, four types of pellets were prepared; one using exhausted olive mill solid waste (G) noted (100G) and three using G blended with pine sawdust (S) in different percentages (50%S–50%G (50S50G); 60%S–40%G (60S40G); 80%S–20%G (80S20G)). Investigations showed that when isothermal temperature increases during the gasification conducted with two water steam percentages of 10% and 30%, the reactivity increases with potassium concentration up to 0.5 M, especially for 100G. Still, higher catalyst concentration (1.5 M) showed adverse effects attributable to silicon release and char pore fouling. Moreover, the effect of the steam concentration on the gasification reactivity was significant with the non-impregnated sample 100G. Finally, a kinetic study was carried out to determine the different kinetic parameters corresponding to the Arrhenius law.

Keywords: catalyst; biofuel; potassium; gasification; waste

Citation: Nsibi, C.; Pozzobon, V.; Escudero-Sanz, J.; Lajili, M. Catalytic Effects of Potassium Concentration on Steam Gasification of Biofuels Blended from Olive Mill Solid Wastes and Pine Sawdust for a Sustainable Energy of Syngas. *Sustainability* **2024**, *16*, 9040. https://doi.org/10.3390/su16209040

Academic Editor: Firoz Alam

Received: 15 September 2024
Revised: 16 October 2024
Accepted: 17 October 2024
Published: 18 October 2024

1. Introduction

Renewable energy is critical to meeting growing energy demand while reducing the negative environmental impact of fossil fuel use. For this purpose, biomass resources such as forestry, agricultural wastes, agrifood byproducts, and municipal wastes can be exploited as alternative fuels [1]. Indeed, due to its abundance and low cost, biomass may represent an interesting and renewable energy source that is environmentally friendly. Nowadays, biomass contributes about 10 to 15% of the world's primary energy consumption [2]. It ranked as the fourth energy source after oil, gas and coal [3,4]. Among the available biomass, wood and olive wastes are at the head of lists in the Mediterranean basin. For example, in Tunisia, the olive wastes produced by the olive oil industry account, depending on pluviometry, about 400,000 tons/year of olive pomace and 1,200,000 tons/year of olive mill wastewater [5,6].

In order to produce heat and or electricity using biomass, it is paramount to select adequate pretreatments (drying and compaction, binder use, and mixing between different types or not) and suitable conversion processes. Currently, combustion [7], pyrolysis [8], and gasification [9] are the most used thermochemical processes [10]. In this context, it turns out that gasification, in comparison with combustion, exhibits many advantages. Indeed, the gasification process has significantly lower pollutant emissions, is

considerably more efficient, and shows a certain flexibility concerning feedstock use. Hence, the syngas product obtained by gasification class this heat process among the best and clean sustainable energy conversion [11,12]. However, the key advantage of choosing this technique is that converting a solid fuel into gas could reach approximately 70–80% of the conservation of the chemical energy contained in the original substance [13]. The so-called syngas yielded, composed mainly of H_2 and CO, can be directly employed as a fuel gas for engines and gas turbines or in chemical syntheses and as solid oxides for fuel cells [14–16].

Gasification can be achieved either using the char obtained by pyrolysis carried out separately from gasification or by a pyrogasification process during which pyrolysis and gasification are performed continuously [17]. In addition, a catalysis protocol could be undertaken to improve the gasification efficiency [18,19]. In fact, the catalytic effects produced by inherent or impregnated alkali and alkaline earth metals were reported in the literature [20,21]. Furthermore, alkali and alkaline earth metals are abundant in raw lignocellulosic biomass and can influence drastically the process outcome [22]. Their frequent use in industrial processes testifies to their availability, low cost, low toxicity, and quality of the products [22,23]. More specifically, alkali metals (potassium and sodium) are more active than alkaline earth [24–26]. In this context, Perander et al. [27] have demonstrated a linear increase in reactivity with a rise in alkali impregnation per kg of biomass, and many reported methods have been used to investigate the effects of these inorganic elements [26]. Researchers have used raw biomass or char impregnated with a solution containing inorganic compounds [25,26]. They compared the effects of different addition methods and concluded that the catalytic effect of K_2CO_3 was more pronounced in impregnation than in dry mixing. Indeed, Dahou et al. [28] concluded that potassium catalyzes high-temperature pyrolysis as well as gasification in a steam gasifier. Therefore, the char reactivity during the gasification process depends not only on the composition and the properties of biomass (percentages of cellulose, hemicellulose, lignin, and inorganic content) [25] but also on the experimental conditions for char formation, such as pyrolysis temperature, the heating rate, and of the operating conditions during gasification (isothermal temperature, the gasifying agent and its partial pressure, and of the residence time) [28].

This experimental study seeks to examine the impact of potassium on the gasification process and the effect of its concentration on conversion rate and reactivity. The novelty of the present work comes from the used biomass and also when trying to find an effect limitation of the inorganic concentration, which will constitute a gain, especially when extending this pilot research to an industrial wide scale. For this goal, three concentrations of aqueous solution of K_2CO_3 were selected for the impregnation of exhausted olive mill solid waste blended or not with pine sawdust. Attention has been devoted to the gasification of char previously produced by pyrolysis of those samples via Thermo Gravimetric Analysis (TGA). The conversion, the conversion rate, and the char reactivity, under different temperature and steam/nitrogen percentages conditions were undertaken and analyzed. The last part of the present study was devoted to modeling. Indeed, developing a model of the substrate behavior paves the way toward large-scale conversion system design. In this case, a kinetic of gasification based on Arrhenius law was chosen. Its characteristic parameters, i.e., the activation energy (Ea), the pre-exponential factor (A), and the reaction order (n), were evaluated.

2. Materials and Methods

2.1. Raw Substrates and Sample Preparation

The selected biomass for this study is olive mill solid wastes collected from the Zouila Oil Press Company situated in the region of Mahdia (Sahel of Tunisia), and the pine sawdust was provided by a wood factory situated in the region of Mulhouse in France. The pellets were prepared following the same experimental procedure previously reported [29]. For the fixed mass, four biomasses were prepared: 80S20G (composed of 80% pine sawdust and 20% olive waste), 60S40G (composed of 60% pine sawdust and 40% olive

waste), 50S50G (composed of 50% pine sawdust and 50% olive waste) and 100G (composed of 100% pure olive waste).

The different samples were first impregnated with potassium with three different solutions of K_2CO_3 (concentrations of 0.1 M, 0.5 M, and 1.5 M).

The biomass submerged in the solution was stirred at 500 rpm for 12 h by an overhead stirrer at room temperature. The ratio of solution to biomass was retained at 16 mL/g to avoid the formation of a layer of the sample at the bottom of the beaker. After impregnation, vacuum filtration has been adopted to recover the final solid mass. In the end, the recovered biomass was dried overnight at 105 °C.

Table 1 displays the results of Inductively Coupled Plasma-Optical Emission Spectroscopy (ICP-OES) analyses realized on the prepared samples for determination of minerals amounts. It is to be highlighted that the mineral analysis of samples 100G and pin sawdust was carried out during a previous study [30], and we included the results recalculated on a dry basis in Table 1. Tables 2–4 list the ultimate analysis, respectively, of each biomass and its corresponding char.

Table 1. ICP-OES analysis of inorganics in the 100G and sawdust pin samples (mg/kg of dry matter).

	Sawdust 100S	**100G**
Na	10	3637
K	1406	17,189
P	64	615
Mn	48	8
Fe	49	197
Mg	113	551
Si	45	416
Ca	1397	5301
Al	34	226

Table 2. ICP-OES analysis of inorganics in the biomass samples (mg/kg of dry matter).

Sample	**80%S/20%G**				**60%S/40%G**				**50%S/50%G**			
Conc.	**NI**	**0.1 M**	**0.5 M**	**1.5 M**	**NI**	**0.1 M**	**0.5 M**	**1.5 M**	**NI**	**0.1 M**	**0.5 M**	**1.5 M**
Al	106	860	95.3	144	132	368	169	423	165	146	1574	213
As	<31	<77	<45	<61	<51	<68	<32	<57	<49	<91	<35	<34
Ca	2231	2033	1857	1496	3687	3138	3038	2651	3612	3391	2803	2229
Cd	<16	<38	<23	<30	<26	<34	<16	<29	<25	<45	<18	<17
Co	<16	66.6	<23	<30	<26	137	<16	<29	<25	<45	<18	<17
Cr	18.4	59.3	60.9	54.4	84	<34	19.9	<29	53.8	<45	24.3	24.5
Cu	<16	<38	<23	<30	<26	<34	<16	<29	<25	<45	<18	<17
Fe	172	558	331	297	447	564	198	208	372	247	265	205
Hg	<63	<154	<91	<122	<102	<135	<65	<115	<98	<182	<71	<69
K	<6250	18,552	46,753	84,945	<10,204	22,111	40,837	84,691	<9804	19,938	38,893	118,968
Mg	312	175	122	103	340	225	156	147	330	236	167	106
Mn	25.7	<38	25.8	<30	25.5	<34	21.6	<29	<49	<45	<18	<17
Mo	<31	<77	<45	<61	<51	<68	<32	<57	<49	<91	<35	<34
Na	524	942	563	742	803	747	358	672	831	951	3275	424
Ni	<31	79.3	<45	<61	<51	99.4	<32	<57	<49	<91	45.3	<34
P	417	913	498	621	566	632	318	546	564	831	360	334
Pb	<31	<77	<45	<61	<51	<68	<32	<57	<49	<91	<35	<34
Sb	<31	<77	<45	<61	<51	<68	<32	<57	<49	<91	<35	<34
Si	928	1287	1037	762	1691	2094	1955	2670	2987	3104	43,754	2064
Ti	<16	<38	<23	<30	<26	<34	<16	<29	<25	<45	22.7	<17
V	<31	<77	<45	<61	<51	<68	<32	<57	<49	<91	<35	<34
Zn	<16	<38	<23	<30	<26	<34	<16	<29	<25	<45	<18	<17

From Table 3, it can be noted that elementary analyses for the other chars are not carried out.

Table 3. Results of measurements of the C. H. N. S. O level in biomass samples (in %).

Samples		N	C	H	S	O
Sawdust 100%G		0.20	51.30	6.40	0.00	41.50
	NI	1.16	46.43	6.38	0.00	46.03 *
	0.1 M	1.21	49.90	6.58	0.00	42.31 *
	0.5 M	0.74	41.54	5.79	0.00	51.93 *
	1.5 M	0.94	29.83	4.05	0.00	65.18 *
80%S–20%G	NI	0.21	45.56	6.38	0.00	47.64
	0.1 M	0.21	43.98	6.21	0.00	46.68
	0.5 M	0.20	41.15	5.88	0.00	43.76
	1.5 M	0.16	37.11	5.10	0.00	40.20
60%S–40%G	NI	0.30	46.20	6.42	0.00	43.84
	0.1 M	0.29	44.30	6.03	0.00	42.70
	0.5 M	0.27	42.02	6.06	0.00	42.90
	1.5 M	0.23	37.81	5.20	0.00	39.86
50%S–50%G	NI	0.35	46.27	6.51	0.00	45.85
	0.1 M	0.34	45.38	6.42	0.00	44.16
	0.5 M	0.29	39.56	5.55	0.00	39.89
	1.5 M	0.23	34.09	4.74	0.00	45.71

* Total oxygen calculated by difference with all other elements.

Table 4. Results of measurement of C. H. N. S. O content in char samples (in %).

Samples		N	C	H	S	O
80%S–20%G	NI	0.39	66.72	3.85	n.r.	25.8
	0.1 M	0.23	60.82	3.59	n.r.	21.5
	0.5 M	0.18	47.98	4.14	n.r.	26.2
	1.5 M	0.11	39.53	3.34	n.r.	26.4

n.r. no result.

2.2. Experimental Methodology

Once prepared, the samples underwent slow pyrolysis in a Macro-ThermoGravimetric reactor, as shown in Figure 1, under a constant heating rate of 10 °C/min until reaching 400 °C temperature. The flow rate of nitrogen N_2 is fixed at 7.8 NL/min. Slow pyrolysis and the final temperature value were selected to obtain a maximal char yield. Afterward, gasification experiments were conducted under two steam concentrations (10% and 30%) at different isothermal temperatures: 750 °C, 850 °C, and 900 °C. From a practical point of view, the sample was placed at the start on a 5 cm diameter tray and raised using a manual crank ((6) in Figure 1) approximately 10 s into the oven (electrically heated to the fixed temperature set in advance). Hence, a temperature gradient varying between 75 and 95 °C/s is imposed in order to promote the formation of syngas. Each test was repeated 3 times for each sample, temperature, and steam pressure. The end of each test is estimated to be completely achieved when the mass loss, measured by the electronic scale (7), is stabilized. The average of 3 repetitions is taken into account during the curves plot.

The biomass gasification process requires the presence of a gasifying agent (air, steam, carbon dioxide) to attack the biochar and produce the syngas. In all generality, during the gasification, five sorts of reactions could occur, as it is summarized below:

- Carbonation

$$C + CO_2 \leftrightarrow 2CO + 172\ \text{kJ/mol} \quad \text{(Boudouard reaction)} \tag{1}$$

$$C + H_2O \leftrightarrow CO + H_2 + 131\ \text{kJ/mol} \quad \text{(water gas reaction)} \tag{2}$$

$$C + 2H_2 \leftrightarrow CH_4 - 72.8\ \text{kJ/mol} \quad \text{(Hydrogasification)} \tag{3}$$

$$C + \tfrac{1}{2}O_2 \rightarrow CO - 111\ \text{kJ/mol} \tag{4}$$

- Oxidation

$$C + O_2 \rightarrow CO_2 - 394\ \text{kJ/mol} \tag{5}$$

$$CO + \frac{1}{2}\,O_2 \rightarrow CO_2 - 284\ \text{kJ/mol} \tag{6}$$

$$CH_4 + 2\,O_2 \leftrightarrow CO_2 + 2H_2O - 803\ \text{kJ/mol} \tag{7}$$

$$H_2 + \tfrac{1}{2}\,O_2 \rightarrow H_2O - 242\ \text{kJ/mol} \tag{8}$$

- Water gas Shift

$$CO + H_2O \leftrightarrow CO_2 + H_2 - 41.2\ \text{kJ/mol} \tag{9}$$

- Methanation

$$2CO + 2H_2 \rightarrow CO_2 + CH_4 - 247\ \text{kJ/mol} \tag{10}$$

$$CO + 3H_2 \leftrightarrow CH_4 + H_2O - 206\ \text{kJ/mol} \tag{11}$$

$$CO_2 + 4\,H_2 \rightarrow CH_4 + 2H_2O - 165\ \text{kJ/mol} \tag{12}$$

- Steam reforming

$$CH_4 + H_2O \leftrightarrow CO + 3H_2 + 206\ \text{kJ/mol} \tag{13}$$

$$CH_4 + \frac{1}{2}O_2 \rightarrow CO + 2H_2 - 36\ \text{kJ/mol} \tag{14}$$

The syngas composition depends on the preferential reactions occurring during gasification, the nature of the char (morphological structure and particle size), and the operating conditions (reactor type, temperature, pressure, composition, and the type of the gasifier, and residence time) [31]. Several studies [32,33] have shown that one of the advantages of gasification via water steam is that it is the best for generating syngas and that the corresponding chemical kinetic is significantly more rapid than that of CO_2. This justifies the choice of steam as a gasifying agent with two partial pressures and under three isothermal temperatures, 750 °C, 850 °C, and 900 °C.

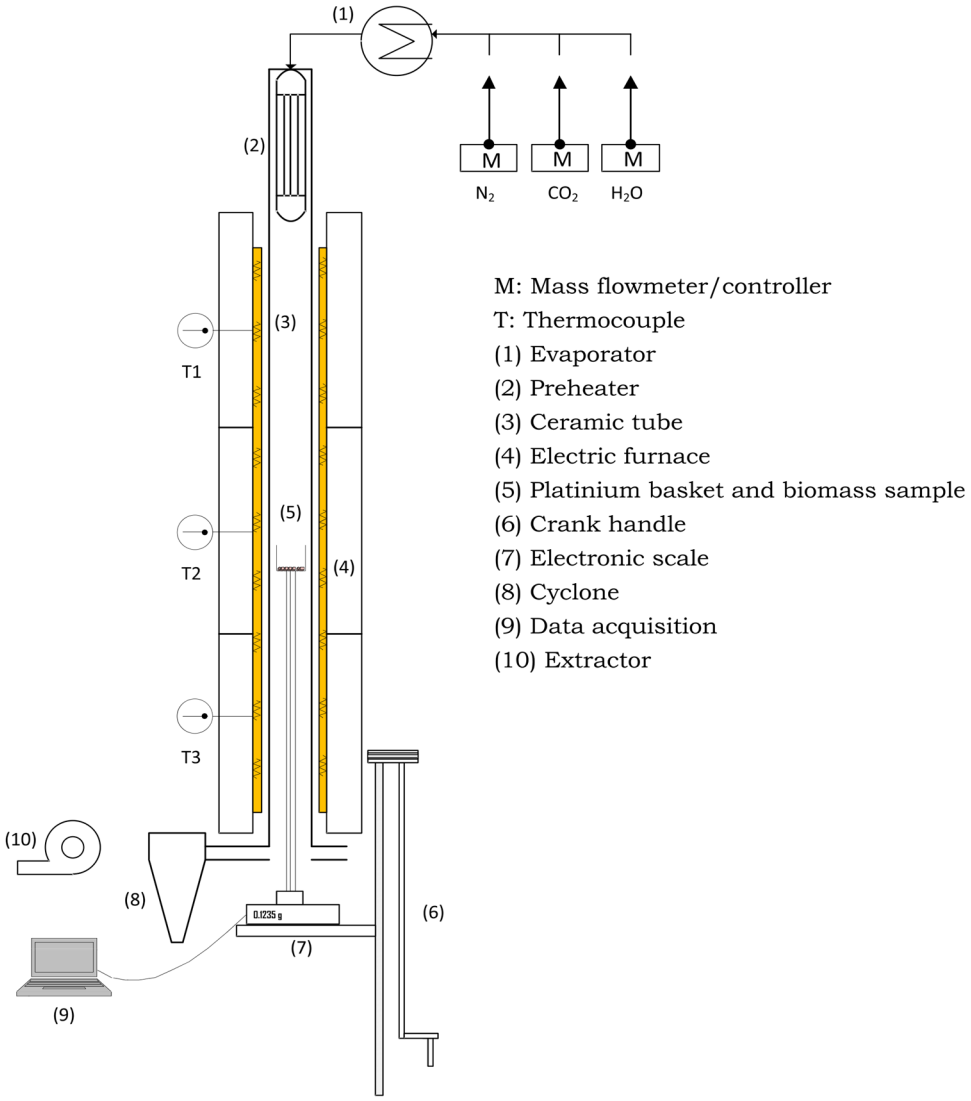

Figure 1. Schematic representation of the M-TG reactor [32].

2.3. Conversion Rate Calculation

The conversion level (X) of char at a given instant 't' can be calculated according to the following expression:

$$X(t) = \frac{m_i - m_t}{m_i - m_f} \quad (15)$$

where m_i is the initial sample mass, $m_t = m(t)$ represents the sample mass measured at time t and m_f indicates the final mass.

The gasification rate is defined as the variation of the conversion versus time:

$$r(t) = \frac{dX}{dt} = \frac{X_{t+1} - X_t}{\Delta t} \quad (16)$$

where Δt is the time difference between two successive instants.

Reactivity data were obtained following the equation [34]:

$$R(X) = \frac{1}{m(t)}\frac{dm(t)}{dt} = \frac{1}{1-X(t)}\frac{dX}{dt} \quad (17)$$

The reactivity at any gasification stage can be expressed as [35,36]:

$$R(X)_{(T,P_i)} = R(X_{ref})_{(T,P_i)}\, f(X) \quad (18)$$

where $f(X)$ is a structural term describing the evolution of char properties, notably the modifications in the number of active sites over the conversion, we assume that this function is independent of the temperature and pressure of the gasifying agent [35,37,38]. $R(X_{ref})$ is a reference reactivity that depends on gas temperature and pressure.

To determine the kinetic parameters, a reference reactivity used at a specific conversion level of char should be considered. Many authors have chosen 10% as the reference conversion value [35]. However, others used an average reactivity between two degrees of conversion [39–41]. In our case, it was chosen not to take a low degree of conversion to avoid error due to the change in the gas composition during the gasification process, nor to take an advanced degree of conversion to avoid neglecting the first gasification stages. Hence, the reference reactivity was set at a level of 50% char conversion (X = 0.5 and $R(X_{ref}) = R(50)$) [35,36]:

By adopting a model of order n based on the Arrhenius model, the reactivity at a 50% conversion level is expressed as follows:

$$R(50)_{(T,P_{H_2O})} = k(T).P_{H_2O}^{n} \quad (19)$$

where $k(T)$ represents the apparent rate constant as a function of temperature (T) and P_{H_2O} is the steam partial pressure.

$$k(T) = A \exp\left(\frac{-E_a}{RT}\right) \quad (20)$$

where A is the pre-exponential factor, E_a is the activation energy, n is the reaction order, and R is the universal gas constant.

3. Results and Discussion

3.1. Effects of Mineral Contents and Potassium Impregnation

Figure 2a shows that the gasification of 50S50G biomass is more rapid than other biomasses in accordance with the results of Lajili et al. [29]. Indeed, the blending process enhances the reactivity of raw biomass up to 50 wt.% of olive waste. Table 1 illustrates the higher potassium content of olive waste compared with sawdust, which accounts for the catalytic effect of potassium on the blended biomass. However, the gasification of 100G biomass is the slowest. This result could be related to the structure of the char and may be to the change in the concentration of inorganic elements having a catalytic or inhibitory effect. It can also be attributable to the presence of aromatic compounds (polyphenol content).

To obtain a better insight into the effect of potassium on the gasification process, the conversion of char of potassium-impregnated biomass at both concentrations (0.1 M and 0.5 M) was represented. It can be seen that the effect of potassium during the gasification of 80S20G char was not significant. Indeed, at t = 600 s, the conversion of this sample is X = 0.93 at T = 750 °C and a steam concentration of 10%. Whereas, after impregnation the conversion becomes X = 0.98 at 0.1 M and X = 0.93 at 0.5 M at the same time and under the same conditions. This could be explained by the saturation of pores of the char when they become covered by a monolayer of catalysts. The same result was found by Bouraoui et al. [42], who explained this saturation by the microporous texture of the char, especially when showing that most pores were plugged for potassium-impregnated samples.

On the other hand, the conversion of other biomasses (50S50G and 60S40G) increased slightly when impregnated with potassium at 0.1 M and decreased very slightly when the concentration of potassium was increased to 0.5 M. Indeed, the conversions of non-impregnated samples 50S50G and 60S40G were X = 0.94 and X = 0.84, respectively, and became X = 0.99 and X = 0.98 for C = 0.1 M and then X = 0.94 and X = 0.95 for C = 0.5 M at the same time (i.e., t = 600 s) and under the same gasification conditions.

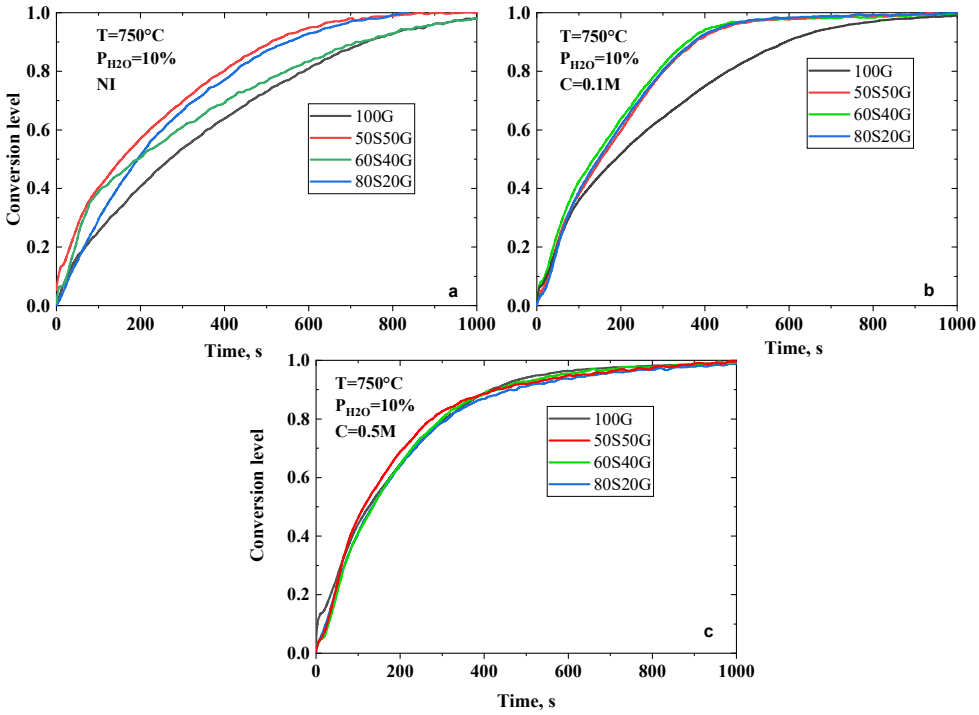

Figure 2. Conversion level versus time for all biomasses: (**a**). Non-impregnated biomasses; (**b**). Impregnated biomasses with C = 0.1 M; (**c**). Impregnated biomasses with C = 0.5 M.

For these biomasses, despite the impregnation, an increase in potassium concentration was not systematically observed because the minerals present in the biomass definitely affect the catalytic activity of potassium. In fact, the elementary analysis of the 50S50G biomass presented in Table 2 shows that by increasing the potassium concentration from 0.1 M to 0.5 M, the silicon content rose from 3104 mg/kg to 43,754 mg/kg dry matter. Thus, given its thermal instability, silicon can react with alkali and alkaline earth metals such as potassium. This can lead to the formation of alkali silicates during the thermochemical transformation of biomass, in turn inhibiting the catalytic activity of potassium [43]. According to the results found by Hognon et al. [44] and Dupont et al. [45], for the case where the potassium concentration is 0.1 M, the K/Si ratio is greater than 1, and the catalytic effect of potassium is highlighted. In contrast, when the potassium concentration increases to 0.5 M, the K/Si ratio becomes less than 1, and the inhibiting effect of silicon is observed during gasification. This effect can be seen more clearly in Figure 3, where it can be noted that the conversion rate is higher when the concentration of potassium is 0.1 M, both for low conversion values ($X < 0.3$) and high conversion values ($X > 0.4$). All this is due to the silicon encapsulation of potassium, limiting its catalytic effect.

The amount of iron contained in the 60S40G sample dropped from 564 mg/kg to 198 mg/kg dry basis when the potassium concentration during impregnation passed from C = 0.1 M to C = 0.5 M. Knowing that iron could play a catalytic role and according to Cortazar et al. [46], it can be concluded that iron catalyzes the gasification of olivine when using a steam gasifier. Moreover, it can be deduced that the optimal value of potassium concentration is 0.1 M at T = 750 °C for 80S20G, 50S50G, and 60S40G, respectively. However, for the 100G sample and under the same gasification conditions, the conversion is found to be X = 0.81 for the non-impregnated sample, X = 0.90 for C = 0.1 M, and X = 0.97 for C = 0.5 M for the same instant t = 600 s. Hence, potassium seems to play a significant catalytic role in enhancing gasification yields, as seen in Figure 4.

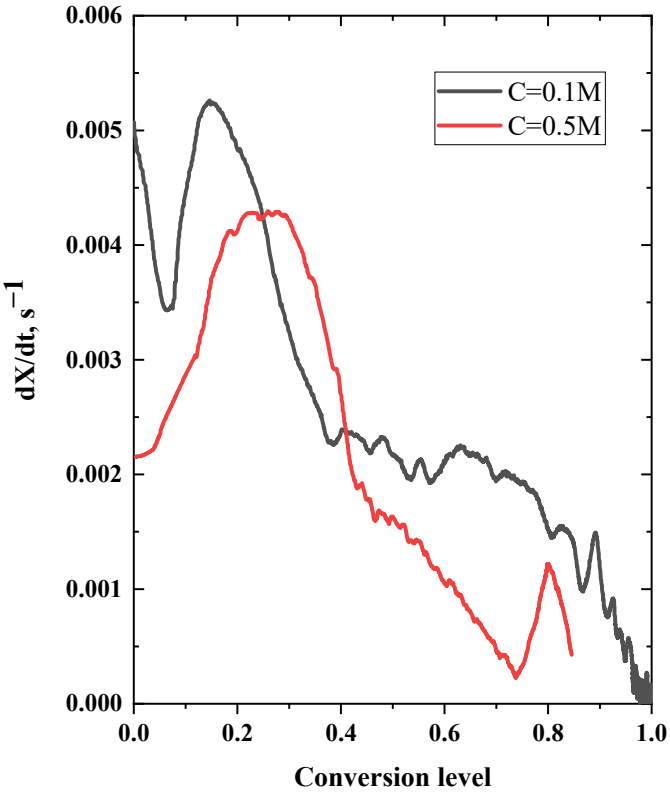

Figure 3. Reaction rate versus conversion in the case of 50S50G.

It should be noted that the conversions of these four samples decrease or are not influenced by increasing the concentration of potassium impregnated at 1.5 M.

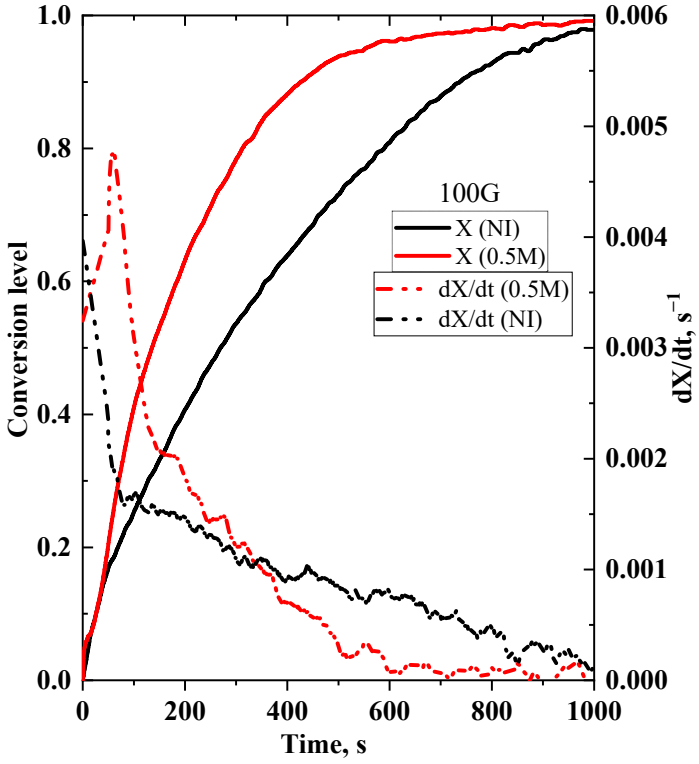

Figure 4. Conversion and reaction rate versus time for 100G (non-impregnated and impregnated biomass with C = 0.5 M) at T = 750 °C.

3.2. Effects of Temperature

The role of temperature in the gasification process can be seen in Figure 5a, which shows 100G when working at temperatures ranging from 750 °C to 900 °C with 10% H_2O. It can be seen that gasification was significantly influenced by increasing temperature. In fact, to reach 90% char conversion, the gasification reaction took 216 s at T = 900 °C, 507 s at T = 850 °C, and 800 s at T = 750 °C, respectively. Therefore, a 150 °C increase in temperature leads to about 4 times greater reactivity. Similarly, Figure 5b, for impregnated samples, shows that an increase in temperature leads to a slight increase in the conversion rate. These findings align with those reported in the literature [32,47]. For the 60S40G sample impregnated at 0.5 M, the same effects of increasing temperature on the reaction rate (Figure 6a) and char reactivity were observed (Figure 6b). More precisely, the reaction rate increased at low conversion (X < 0.5) and then decreased in agreement with Elsaddik et al. [48], who suggest that at high conversion, when carbon is consumed, the silicon concentration in the char rises, inducing to a decrease in the reaction rate. The same behavior was observed for the 50S50G sample shown in Figure 7. Indeed, to reach a conversion rate of 30%, the reaction rate rose from 0.003 s^{-1} at T = 750 °C to 0.009 s^{-1} at T = 900 °C.

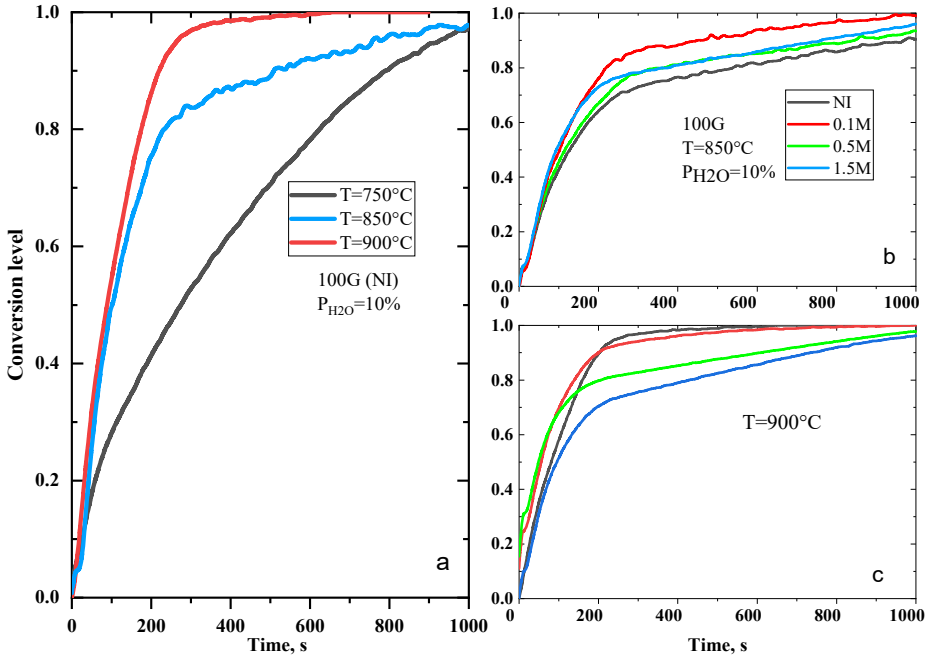

Figure 5. (**a**) Conversion versus reaction time for non-impregnated sample ; (**b**,**c**) impregnated sample.

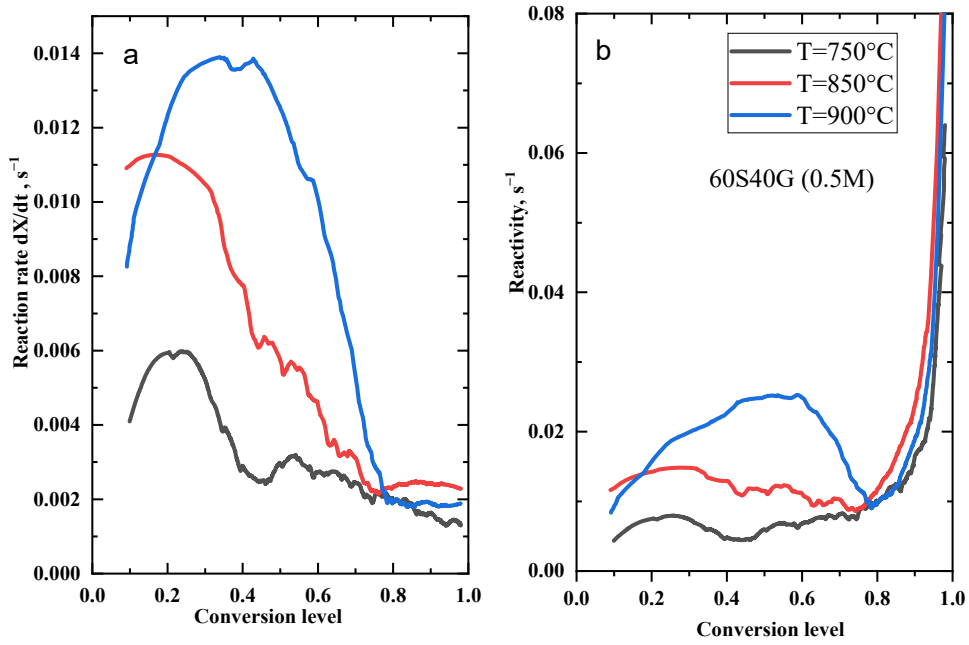

Figure 6. (**a**) Reaction rate versus conversion and (**b**) Char reactivity as a function of conversion.

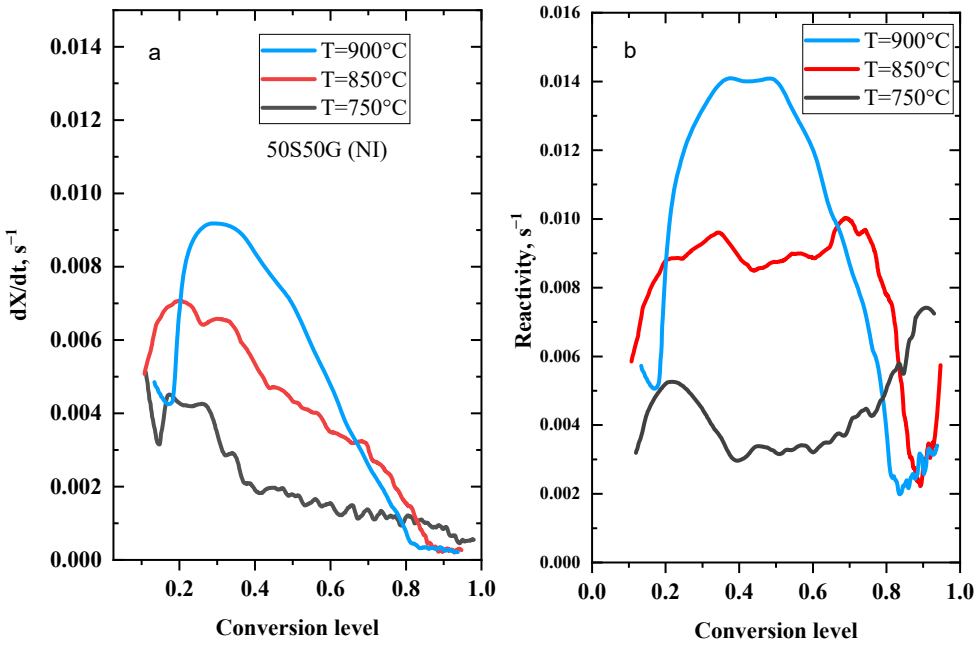

Figure 7. (**a**) Reaction rate as a function of conversion for 50S50G at different temperatures with 10% H_2O and (**b**) Reactivity versus conversion for the same sample.

3.3. Effects of Steam Percentage

The partial pressure of H_2O was increased from 10% to 30% at 850 °C. Figure 8a shows that 10% H_2O enhances the gasification of impregnated samples with K_2CO_3 0.1 M compared with non-impregnated 100G, whereas 30% H_2O shows a contrary effect for the same sample, as illustrated in Figure 8b. Hence, with impregnated samples, an increase in partial pressure steam leads to decreased char reactivity during gasification. Furthermore, to reach 90% char conversion under 10% H_2O with non-impregnated 100G, 1000 s are needed, whereas it takes only 161 s when working under 30% H_2O at the same temperature. Hence, gasification of 90% char conversion is 6.2 times faster with 30% H_2O than with 10% H_2O for non-impregnated 100G. Moreover, Figure 9a,b shows that an increase in

steam partial pressure leads to an increase in char reactivities. More precisely, the reactivity increases, especially since the conversion progresses (it suddenly rises for X > 0.8). These results are in line with those reported in the literature. For example, Mermoud et al. [49] and Tagutchou et al. [50] have observed an increase in the ratio of 1.9 and 3 between partial steam pressures of 10% and 40%. In the same way, Marwa et al. [51] proved that when increasing the percentage of water steam from 10 to 20%, the conversion rate was significantly enhanced in the case of impregnated sawdust with olive mill wastewater.

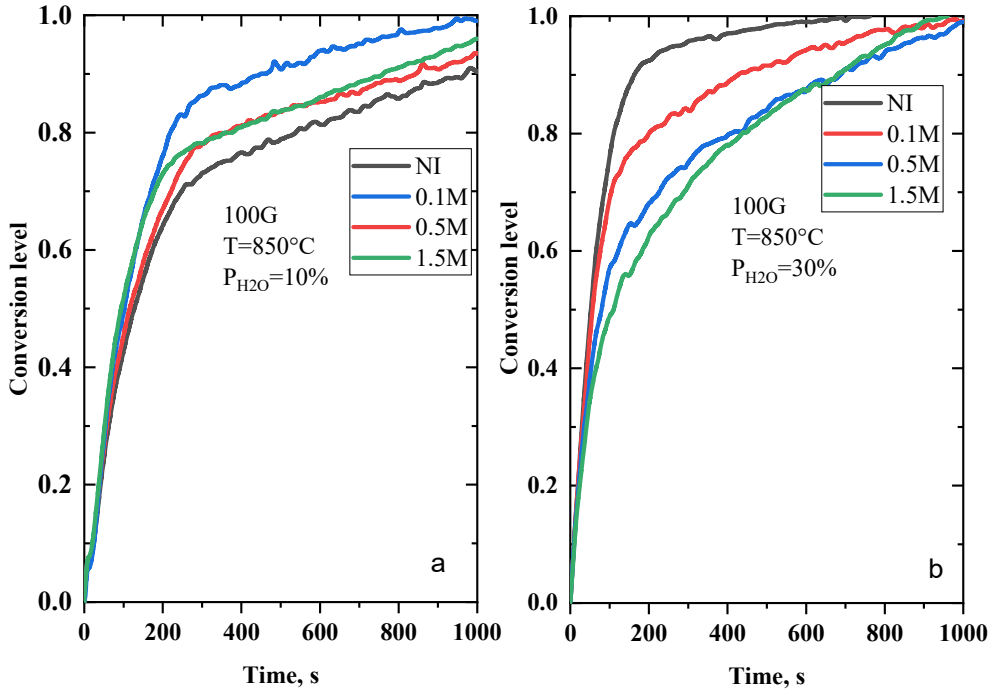

Figure 8. (**a**) Conversion versus reaction time for 100G with 10% H_2O and (**b**) with 30% H_2O.

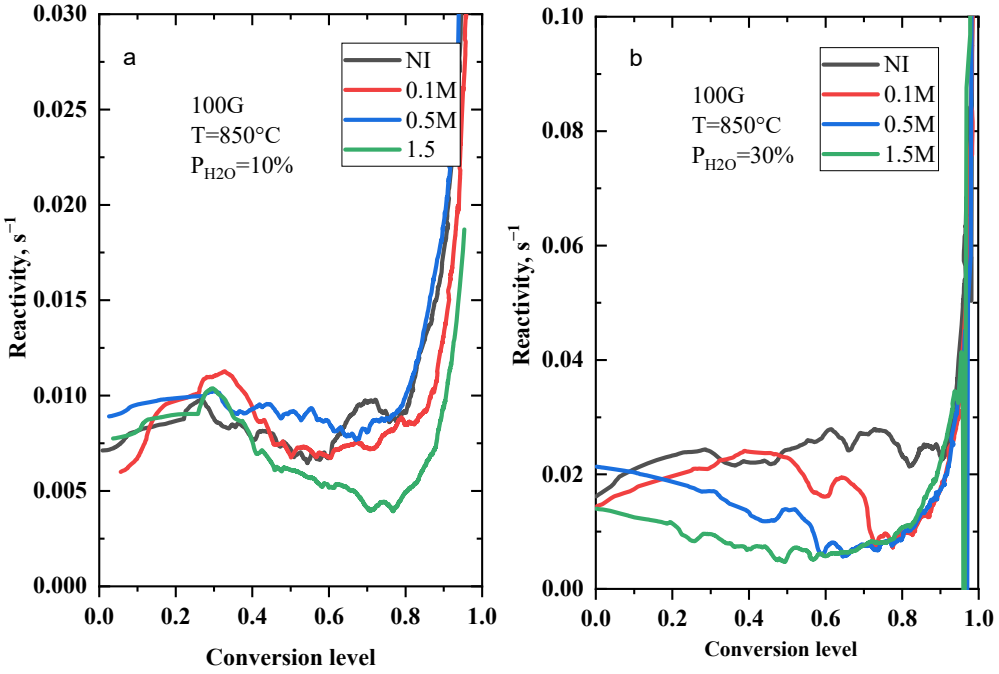

Figure 9. (**a**) Reactivity profile of 100G versus conversion with 10% H_2O and (**b**) with 30% H_2O.

To apprehend the thermal degradation during the gasification process and the effect of potassium impregnation, a kinetic study based on the Arrhenius law is necessary in order to determine crucial kinetic parameters such as the activation energy (E_a), which indicates the minimum energy required for chemical bond breaking, the reaction order (n) and the pre-exponential factor (A) which corresponds to the frequency of collisions between molecules in a chemical reaction.

3.4. Determination of Kinetic Parameters

Applying logarithm to both sides of Equation (19) is recommended. Then, using a least-squares linear regression method allows us to obtain a best-fit straight line from each curve showing $\ln R_{50}$ versus 1/T and those of $\ln R_{50}$ as a function of Ln (p). From the slope of the curve $\ln R_{50}$ as a function of 1/T, the activation energy was determined. Then, from the curve representing $\ln R_{50}$ as a function of Ln (p), the order of the reaction was obtained. Finally, the pre-exponential coefficient was deduced from the ordinate of the linear curve at the origin.

Figures 10–12 illustrate Arrhenius plots for the studied gasification process, with steam partial pressures of 10% and 30% and temperatures of 750 °C, 850 °C, and 900 °C, respectively. It can be noted that as the temperature increases, the reactivity increases. It is worth noting that these curves show an opposite trend for 0.1 M of potassium concentration when compared with other high concentrations. Indeed, gasification is a complex process influenced by three factors: catalyst, temperature, and partial steam pressure, respectively. As shown in these figures, it seems that these factors act on opposite sides, and it remains to be seen who prevails over others. Kinetic parameters are summarized in Table 5. More particularly, for the 50S50G and 80S20G samples, as the K_2CO_3 increases, the activation energy decreases, which is in accordance with reported previous results [35]. The latter authors concluded that the lowest activation energies are attributable to chars with the highest potassium contents. However, the activation energies of 100G found in the present work, varying between 66.981 and 46.293 kJ/mol, are lower than those found by Lampropoulos et al. [19] during gasification of olive kernel under CO_2 (varying between 140 kJ/mol to 170 kJ/mol). In addition, Elorf et al. [52] found activation energies with raw solid residue without oil during steam gasification ranged between 77.2 and 71.1 kJ/mol. The relatively small activation energies found in this work could be explained by the high potassium content in the four samples and the fairly mild pyrolysis conditions (i.e., the different degrees of graphitization of the chars). Nevertheless, it should be highlighted that the negative value of the activation energy of the sample has no physical meaning. However, it may be due to measurement fluctuations at the phases of the start tests. Besides, it can be concluded that kinetic constants, in this case, are independent of temperature. In this context, several authors have found a negative activation energy [53–55]. Indeed, Müller, R et al. [54] treated the steam gasification of coal exposed to higher flux irradiation, and they explained the negative sign of the activation energy by the fact that it does not necessarily imply an inconsistency with the theory, but it depends on the different kind of the elementary reactions of the complex gasification process.

Table 5. Kinetic parameters of different samples.

Samples		E_a(kJ/mol)	R^2	Reaction Order (n)	A (s^{-1})
100G	NI	62.981	0.996	0.936	32.927×10^0
	C = 0.1 M	66.676	0.983	0.528	72.469×10^0
	C = 0.5 M	46.293	0.939	0.276	1.594×10^0
	C = 1.5 M	60.022	0.933	−0.063	4.041×10^0
50S50G	NI	74.098	0.627	0.413	11.5853×10^1
	C = 0.1 M	62.787	0.740	−0.574	3.482×10^0
	C = 0.5 M	60.434	0.610	0.131	9.895×10^0
	C = 1.5 M	−70.777	0.962	−0.052	2.923×10^5
80S20G	NI	133.721	0.999	−0.671	4.700×10^3

C = 0.1 M	28.754	0.957	−0.583	73.196×10^{-3}
C = 0.5 M	23.937	0.905	−0.059	74.507×10^{-3}
C = 1.5 M	1.697	0.703	0.619	33.357×10^{-3}

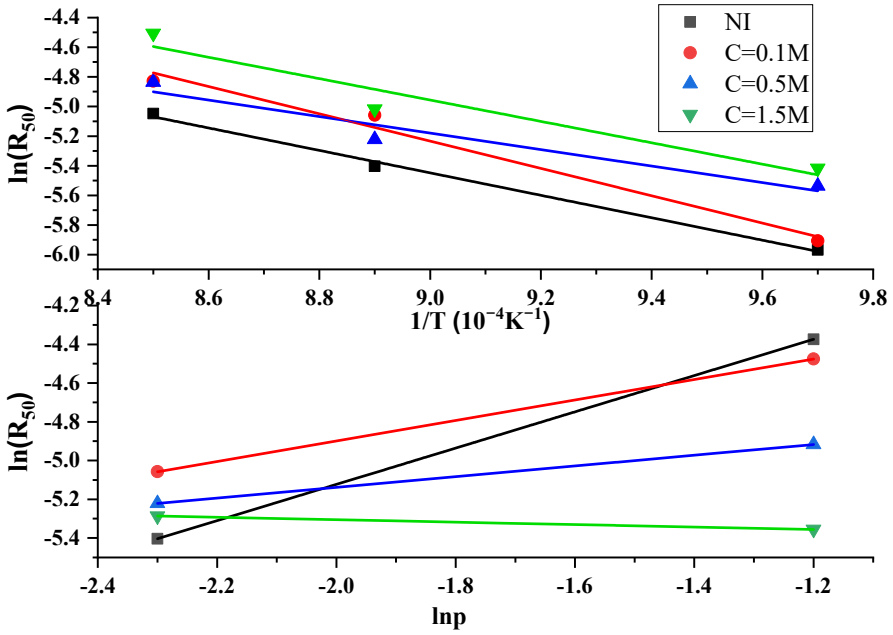

Figure 10. Arrhenius plots of ln(R50) versus 1/T and ln(R50) versus ln(p) for 100G.

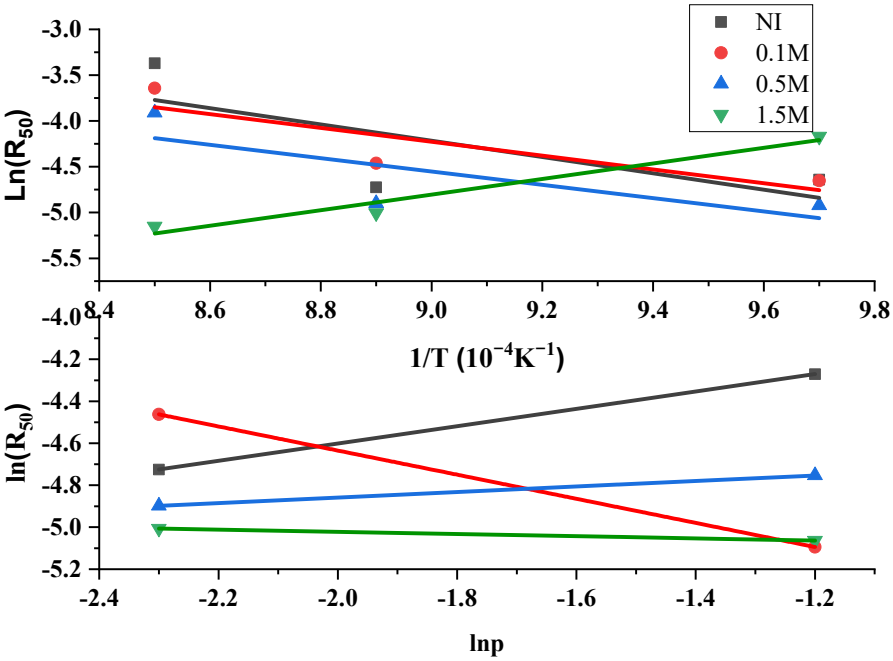

Figure 11. Arrhenius plots of ln(R50) versus 1/T and ln(R50) versus ln(p) for 50S50G.

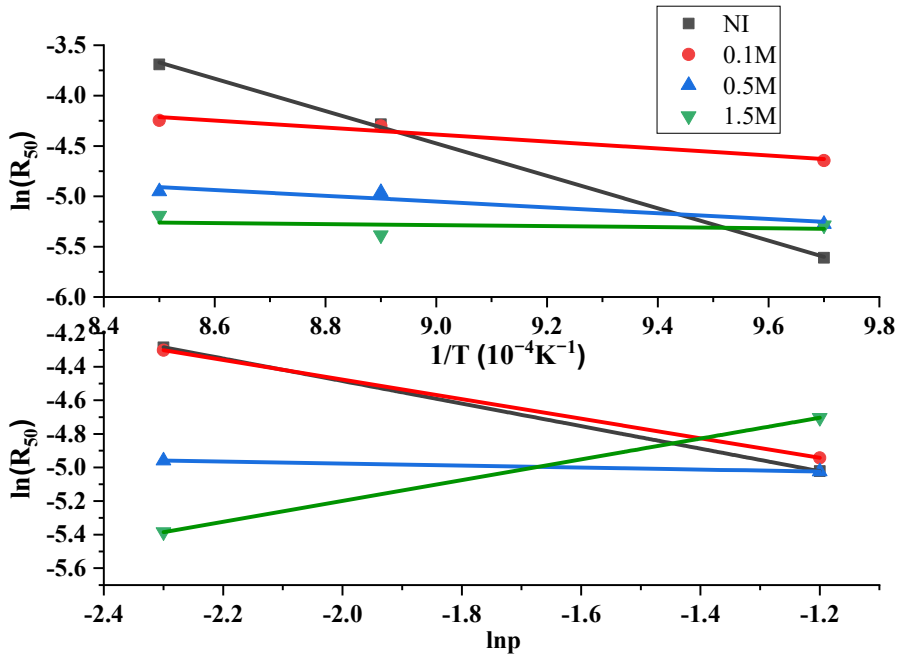

Figure 12. Arrhenius plots of ln(R50) versus 1/T and ln(R50) versus ln(p) for 80S20G.

4. Conclusions

The present work contributes to the understanding of the role of potassium in char gasification using steam as the gasifying agent. Special attention was given to the effect of the potassium catalysis effect via K_2CO_3 with different concentrations. The chosen gasification process is conducted under different temperatures and steam partial pressures. Results show that operating conditions clearly affect the reactivity of the chars depending on potassium concentration:

(1) As for the impact of temperature, we noticed that there was an increase in reactivity up to 4 times just by increasing the temperature by 150 °C.
(2) The increase in steam pressure also had a remarkable effect on the gasification process of the different samples, especially on the 100G NI sample, whose conversion and reactivity profiles were considerably influenced by this increase.
(3) It can also be concluded that the inorganic elements, such as iron and silicon, could play a concurrent role with potassium by activating or inhibiting the gasification process.
(4) K_2CO_3 concentration of 0.5 M could be considered the most efficient molarity for impregnation in the case of 100G and 0.1 M for the other samples with well-defined conditions of steam pressure and temperature.
(5) Characteristic parameters of Arrhenius law were determined for all samples for the reference reactivity of 50% conversion. The activation energies of our samples, especially of 100G, are lower than those found in reported works in the literature, indicating the crucial role of potassium during catalysis.

This study will be supplemented by a morphological study of the chars of the various samples to comprehend better the interaction of the impregnated potassium atoms with the char surfaces.

Author Contributions: Methodology, C.N., J.E.-S. and M.L.; Formal analysis, C.N., J.E.-S. and M.L.; Investigation, C.N.; Writing—original draft, C.N.; Writing—review & editing, V.P., J.E.-S. and M.L.; Supervision, J.E.-S. and M.L.; Project administration, M.L.; Funding acquisition, M.L. All authors have read and agreed to the published version of the manuscript.

Funding: Communauté urbaine du Grand Reims, Département de la Marne, Région Grand Est, and European Union (FEDER Champagne-Ardenne 2014–2020) are acknowledged for their financial

support to the Chair of Biotechnology of CentraleSupélec and the Centre Européen de Biotechnologie et de Bioéconomie (CEBB).

Institutional Review Board Statement: Not applicable.

Informed Consent Statement: Not applicable.

Data Availability Statement: Data are contained within the article.

Conflicts of Interest: The authors declare no conflicts of interest.

References

1. Anvari, S.; Aguado, R.; Jurado, F.; Fendri, M.; Zaier, H.; Larbi, A.; Vera, D. Analysis of agricultural waste/byproduct biomass potential for bioenergy: The case of Tunisia. *Energy Sustain. Dev.* **2024**, 78, 101367.
2. World Bioenergy Association. *Statistics, Global Bioenergy*; World Bioenergy Association: Stockholm, Sweden, 2020.
3. Nunes Leonel, J.R. Biomass gasification as an industrial process with effective proof-of-concept: A comprehensive review on technologies, processes and future developments. *Results Eng.* **2022**, *14*, 100408.
4. García, R.; Pizarro, C.; Lavín, A.G.; Bueno, J.L. Characterization of Spanish biomass wastes for energy use. *Bioresour. Technol.* **2012**, *103*, 249–258.
5. Saidur, R.; Abdelaziz, E.A.; Demirbas, A.; Hossain, M.S.; Mekhilef, S. A review on biomass as a fuel for boilers. *Renew. Sustain. Energy Rev.* **2011**, *15*, 2262–2289.
6. Elkadri, A.; Elfkih, S.; Sahnoun, H.; Abichou, M. Storage tanks' olive mill wastewater management in Tunisia. *Sustain. Water Resour. Manag.* **2022**, *8*, 1.
7. Jenkins, B.M.; Baxter, L.L.; Miles Jr, T.R.; Miles, T.R. Combustion properties of biomass. *Fuel Process. Technol.* **1998**, *54*, 17–46.
8. Yaman, S. Pyrolysis of biomass to produce fuels and chemical feedstocks. *Energy Convers. Manag.* **2004**, *45*, 651–671.
9. Molino, A.; Chianese, S.; Musmarra, D. Biomass gasification technology: The state of the art overview. *J. Energy Chem.* **2016**, *25*, 10–25.
10. Sutton, D.; Kelleher, B.; Ross, J.R. Review of literature on catalysts for biomass gasification. *Fuel Process. Technol.* **2001**, *73*, 155–173.
11. Fung, D.P.C.; Kim, S.D. Gasification kinetics of coals and wood. *Korean J. Chem. Eng.* **1990**, *7*, 109–114.
12. Park, J.H.; Park, H.W.; Choi, S.; Park, D.W. Effects of blend ratio between high density polyethylene and biomass on co-gasification behavior in a two-stage gasification system. *Int. J. Hydrog. Energy* **2016**, *41*, 16813–16822.
13. Lahijani, P.; Zainal, Z.A.; Mohammadi, M.; Mohamed, A.R. Conversion of the greenhouse gas CO_2 to the fuel gas CO via the Boudouard reaction: A review. *Renew. Sustain. Energy Rev.* **2015**, *41*, 615–632.
14. Beagle, E.; Wang, Y.; Bell, D.; Belmont, E. Co-gasification of pine and oak biochar with sub-bituminous coal in carbon dioxide. *Bioresour. Technol.* **2018**, *251*, 31–39.
15. Vamvuka, D.; Teftiki, A.; Sfakiotakis, S. Increasing the reactivity of waste biochars during their co-gasification with carbon dioxide using catalysts and bio-oils. *Thermochim. Acta* **2021**, *704*, 179015.
16. Ricoul, F. Association D'un Procédé de Gazéification Avec Une Pile à Combustion Haute Température (SOFC) Pour La Production D'électricité à Partir de Biomasse. Ph.D. Thesis, Nantes Université, Nantes, France, 2016.
17. Hervy, M. Valorisation de chars issus de pyrogazéification de biomasse pour la purification de syngas: Lien entre propriétés physico-chimiques, procédé de fonctionnalisation et efficacité du traitement. Ph.D. Thesis, Ecole Nationale des Mines d'Albi-Carmaux, Albi, France, 2016.
18. Chin, B.L.F.; Yusup, S.; Al Shoaibi, A.; Kannan, P.; Srinivasakannan, C.; Sulaiman, S.A.; Herman, A.P. Effect of temperature on catalytic steam co-gasification of rubber seed shells and plastic HDPE residues. *Chem. Eng. Trans.* **2016**, *52*, 577–582.
19. Lampropoulos, A.; Kaklidis, N.; Athanasiou, C.; Montes-Morán, M.A.; Arenillas, A.; Menéndez, J.A.; Binas, V.D.; Konsolakis, M.; Marnellos, G.E. Effect of Olive Kernel thermal treatment (torrefaction vs. slow pyrolysis) on the physicochemical characteristics and the CO_2 or H_2O gasification performance of as-prepared biochars. *Int. J. Hydrog. Energy* **2021**, *46*, 29126–29141.
20. Peres, A.P.; Lunelli, B.H.; Maciel FIlho, R. Application of biomass to hydrogen and syngas production. *Chem. Eng. Trans.* **2013**, *32*, 589–594.
21. Sandvik, P. High-Pressure Natural Gas to Syngas Chemical Looping: Thermodynamic Modeling, Gas-to-Liquid Plant Integration, and Variable Reducer-Combustor Operating Pressure. Master's Thesis, The Ohio State University, Columbus, OH, USA, 2019.
22. Zhu, C.; Maduskar, S.; Paulsen, A.D.; Dauenhauer, P.J. Alkaline-Earth-Metal-Catalyzed Thin-Film Pyrolysis of Cellulose. *ChemCatChem* **2016**, *8*, 818–829.
23. Nzihou, A.; Stanmore, B.; Sharrock, P. A review of catalysts for the gasification of biomass char, with some reference to coal. *Energy* **2013**, *58*, 305–317.
24. Zhang, Z.H.; Song, Q.; Yao, Q.; Yang, R.M. Influence of the atmosphere on the transformation of alkali and alkaline earth metallic species during rice straw thermal conversion. *Energy Fuels* **2012**, *26*, 1892–1899.
25. Wang, W.; Lemaire, R.; Bensakhria, A.; Luart, D. Review on the catalytic effects of alkali and alkaline earth metals (AAEMs) including sodium, potassium, calcium and magnesium on the pyrolysis of lignocellulosic biomass and on the co-pyrolysis of coal with biomass. *J. Anal. Appl. Pyrolysis* **2022**, *163*, 105479.

26. Huang, Y.; Yin, X.; Wu, C.; Wang, C.; Xie, J.; Zhou, Z.; Li, H. Effects of metal catalysts on CO_2 gasification reactivity of biomass char. *Biotechnol. Adv.* **2009**, *27*, 568–572.
27. Kramb, J.; DeMartini, N.; Perander, M.; Moilanen, A.; Konttinen, J. Modeling of the catalytic effects of potassium and calcium on spruce wood gasification in CO_2. *Fuel Process. Technol.* **2016**, *148*, 50–59.
28. Dahou, T.; Defoort, F.; Jeguirim, M.; Dupont, C. Towards understanding the role of K during biomass steam gasification. *Fuel* **2020**, *282*, 118806.
29. Lajili, M.; Limousy, L.; Jeguirim, M. Physico-chemical properties and thermal degradation characteristics of agropellets from olive mill byproducts/sawdust blends. *Fuel Process. Technol.* **2014**, *126*, 215–221.
30. Kraiem, N.; Jeguirim, M.; Limousy, L.; Lajili, M.; Dorge, S.; Michelin, L.; Said, R. Impregnation of olive mill wastewater on dry biomasses: Impact on chemical properties and combustion performances. *Energy* **2014**, *78*, 479–489.
31. Zhang, Y.; Wan, L.; Guan, J.; Xiong, Q.A.; Zhang, S.; Jin, X. A review on biomass gasification: Effect of main parameters on char generation and reaction. *Energy Fuels* **2020**, *34*, 13438–13455.
32. Guizani, C.; Escudero Sanz, F.J.; Salvador, S. The gasification reactivity of high-heating-rate chars in single and mixed atmospheres of H_2O and CO_2. *Fuel* **2013**, *108*, 812–823.
33. Tagutchou, J.P.; Escudero Sanz, F.J.; Salvador, S. Gasification of woodchip particles: Experimental and numerical study of char–H_2O, char–CO_2, and char–O_2 reactions. *Chem. Eng. Sci.* **2011**, *66*, 4499–4509.
34. Laurendeau, N.M. Heterogeneous kinetics of coal char gasification and combustion. *Prog. Energy Combust. Sci.* **1978**, *4*, 221–270.
35. Ollero, P.; Serrera, A.; Arjona, R.; Alcantarilla, S. The CO2 gasification kinetics of olive residue. *Biomass Bioenergy* **2003**, *24*, 151–161.
36. Gómez-Barea, A.; Ollero, P.; Fernández-Baco, C. Diffusional effects in CO_2 gasification experiments with single biomass char particles. 1. *Exp. Investig. Energy Fuels* **2006**, *20*, 2202–2210.
37. DeGroot, W.F.; Shafizadeh, F. Kinetics of gasification of Douglas Fir and Cottonwood chars by carbon dioxide. *Fuel* **1984**, *63*, 210–216.
38. Gjernes, E.; Fjellerup, J.; Olsen, A. *Combustion and Gasification of Coal and Straw under Pressurized Conditions*; Forskningscenter Risoe: Roskilde, Denmark, 1995.
39. Chen, G.; Yu, Q.; Sjöström, K. Reactivity of char from pyrolysis of birch wood. *J. Anal. Appl. Pyrolysis* **1997**, *40*, 491–499.
40. Stoltze, S.; Henriksen, U.; Lyngbech, T.; Christensen, O. Gasification of straw in a large-sample TGA. In *Nordic Seminar on Solid Fuel Reactivity*; Chalmers University of Technology: Gothenburg, Sweden, 1993; Volume 24.
41. Kan, T.; Strezov, V.; Evans, T.J. Lignocellulosic biomass pyrolysis: A review of product properties and effects of pyrolysis parameters. *Renew. Sustain. Energy Rev.* **2016**, *57*, 1126–1140.
42. Bouraoui, Z.; Dupont, C.; Jeguirim, M.; Limousy, L.; Gadiou, R. CO_2 gasification of woody biomass chars: The influence of K and Si on char reactivity. *Comptes Rendus. Chim.* **2016**, *19*, 457–465.
43. Jacob, S.; Perez, D.D.S.; Dupont, C.; Commandré, J.M.; Broust, F.; Carriau, A.; Sacco, D. Short rotation forestry feedstock: Influence of particle size segregation on biomass properties. *Fuel* **2013**, 111, 820–828.
44. Hognon, C.; Dupont, C.; Grateau, M.; Delrue, F. Comparison of steam gasification reactivity of algal and lignocellulosic biomass: Influence of inorganic elements. *Bioresour. Technol.* **2014**, *164*, 347–353.
45. Dupont, C.; Jacob, S.; Marrakchy, K.O.; Hognon, C.; Grateau, M.; Labalette, F.; Perez, D.D.S. How inorganic elements of biomass influence char steam gasification kinetics. *Energy* **2016**, *109*, 430–435.
46. Cortazar, M.; Santamaria, L.; Lopez, G.; Alvarez, J.; Amutio, M.; Bilbao, J.; Olazar, M. Fe/olivine as primary catalyst in the biomass steam gasification in a fountain confined spouted bed reactor. *J. Ind. Eng. Chem.* **2021**, *99*, 364–379.
47. Zribi, M.; Lajili, M.; Escudero Sanz, F.J. Gasification of biofuels blended from olive mill solid wastes and pine sawdust under different carbon dioxide/nitrogen atmospheres. *Fuel* **2020**, *282*, 118822.
48. Elsaddik, M.; Nzihou, A.; Delmas, M.; Delmas, G.H. Steam gasification of cellulose pulp char: Insights on experimental and kinetic study with a focus on the role of silicon. *Energy* **2023**, *271*, 126997.
49. Mermoud, F. Gazéification de Charbon de Bois à La Vapeur d'eau: De La Particule Isolée Au Lit Fixe Continu. Ph.D. Thesis, Institut National Polytechnique de Toulouse, Toulouse, France, 2006.
50. Tagutchou, J.P. Gazéification du charbon de plaquettes forestières: Particule isolée et lit fixe continu. Ph.D. Thesis, Université de Perpignan, Perpignan, France, 2008.
51. Zribi, M.; Lajili, M.; Escudero Sanz, F.J. Hydrogen enriched syngas production via gasification of biofuels pellets/powders blended from olive mill solid wastes and pine sawdust under different water steam/nitrogen atmospheres. *Int. J. Hydrog. Energy* **2019**, *44*, 11280–11288.
52. Elorf, A.; Kandasamy, J.; Belandria, V.; Bostyn, S.; Sarh, B.; Gökalp, I. Heating rate effects on pyrolysis, gasification and combustion of olive waste. *Biofuels* **2021**, *12*, 1157–1164.
53. Bernardo, C.A.; Trimm, D.L. The kinetics of gasification of carbon deposited on nickel catalysts. *Carbon* **1979**, 17, 115–120.
54. Müller, R.; Zedtwitz, P.V.; Wokaun, A.; Steinfeld, A. Kinetic investigation on steam gasification of charcoal under direct high-flux irradiation. *Chem. Eng. Sci.* **2003**, *58*, 5111–5119.
55. Ariffen, A.R.; Yusoff, N. Kinetic analysis of co-pyrolysis of biomass/sorbent mixtures at different ratios. *IOP Conf. Ser. Mater. Sci. Eng.* **2020**, *778*, 012117.